Journal of The Electrochemical Society

The Electrochemistry of Amorphous Si-B Thin Film Electrodes in Li Cells

The Electrochemistry of Amorphous Si-B Thin Film Electrodes in Li Cells

Hui Liu,[a,b] Min Zhu,[a] Zhijia Du,[c,*] and M. N. Obrovac[b,c,d,,z]**

[a]*School of Materials Science and Engineering, South China University of Technology, Key Laboratory of Advanced Energy Storage Materials of Guangdong Province, Guangzhou 510640, People's Republic of China*
[b]*Department of Chemistry, Dalhousie University, Halifax, N.S. B3H 4R2, Canada*
[c]*Department of Physics and Atmospheric Science, Dalhousie University, Halifax, N.S. B3H 4R2, Canada*
[d]*Institute for Research in Materials, Dalhousie University, Halifax, N.S. B3H 4R2, Canada*

$Si_{1-x}B_x$ thin films of $0.071 \leq x \leq 0.950$ have been synthesized using combinational sputtering. All $Si_{1-x}B_x$ film compositions had a highly amorphous structure consisting of amorphous Si and B phases, as characterized by X-ray diffraction. In Li cells, it was found that all of the Si is active and the B is inactive with lithium. Otherwise, the $Si_{1-x}B_x$ films have similar characteristics as pure Si film electrodes in Li cells, except with reduced capacity due to the added B. However, shifts in the voltage curves appear when the B content is increased that may be induced by stress-voltage coupling between the active Si and the inactive B phases.

Manuscript submitted September 2, 2015; revised manuscript received October 16, 2015. Published November 14, 2015.

Si is considered to be a promising negative electrode for lithium ion batteries because of its high capacity (2194 Ah/L, 3579 mAh/g,[1–2] low average voltage (~0.4 V vs. Li/Li^+),[3] and good thermal stability.[4] However, a major challenge of using Si as a negative electrode is its large volume expansion during lithiation, which can lead to rapid capacity fade. During the past decade, extensive investigations on binary Si-M alloys have been conducted to improve electrochemical performance of Si-based Li-ion anodes. Some work has been reported on Si-M alloys where M is an active metal with lithium, such as Ag, Zn, or Sn.[5–9] Work on nanostructured Si-M alloys where M is a transition metal that is inactive with lithium has also been widely reported, such as Si-Fe, Si-Mn or Si-Co.[10–15] These alloys have been found to be in the form of active Si in a matrix of inactive Si_xM_y. The Si_xM_y phase can dilute of the volume expansion of active Si during lithiation and prevent the aggregation of Si. This can result in Si-based alloys with increased cycling performance. In addition, we have recently reported that the voltage curve of Si in such active/inactive alloys can be shifted by hundreds of millivolts, presumably due to the stress induced by the active Si phase expanding while bonded to the inactive phase.[16]

In contrast to various studies on Si-metal alloys, few studies exist for Si-B alloys. B is a metalloid and is a well-known *p*-type dopant in Si. Rousselot et al. have shown that the electrical conductivity of Si particles could be increased by doping with up to 14.3% B using high-energy ball milling.[17] However, they observed no difference in capacity or rate performance as compared to pure Si. Netz et al. reported SiB_3 as a Li-ion anode, having 440 mAh/g reversible capacity.[18–19] However, there is no mention in the study by Netz et al. of where the SiB_3 was obtained from, and diffraction patterns are not shown. Confirmation of their results is needed. R. Yi et al. reported that rate capability of Si-C composition can be improved by B-doping.[20] No other reports could be found for Si-B alloys as Li-ion negative electrodes and therefore it remains unclear whether B forms an inactive or active phase in Si alloys. Therefore, it is significant to investigate systematically the effect of B content on the structure and electrochemistry of Si-B alloys.

Combinatorial sputtering has been used successfully as a high throughput method to synthesize samples covering a large wide range of stoichiometries and characterize them in Li cells.[21–23] Here, $Si_{1-x}B_x$ thin films with $0.071 \leq x \leq 0.950$ were prepared by combinatorial sputtering and studied as negative electrode materials for Li-ion batteries.

Experimental

$Si_{1-x}B_x$ thin films were synthesized by magnetron sputtering using a modified Corona Vacuum Coater's (Vancouver, BC, Canada) V3T system, which is equipped with a 500 L/s turbo pump and a Polycold system. The chamber pressure was maintained at about 1.0 mTorr argon during the deposition. 50 mm diameter targets of Si (99.9% purity, Pure Tech,) and B (99.5% purity, Kurt J. Lesker) were used. For sputtering, 110 W and 150 W DC powers were supplied to Si and B targets, respectively, and the targets were covered with masks designed to obtain different compositional ranges. All libraries were sputtered for 6 hours.

$Si_{1-x}B_x$ films were deposited on Cu foil disks (Furukawa Electric Co., Japan) with an area of 12.7 mm^2 using as test electrodes. The loading mass of $Si_{1-x}B_x$ varied in a linear with the Cu disks position, and was measured by weighing of Cu disk with a Sartorious SE-2 microbalance (0.1 μg precision) before and after sputter deposition. XRD of films deposited on Si (111) wafers were measured using a Bruker AXS D8 Discover XRD system equipped with a Cu target and a Cu-K_α monochromator. Films deposited on a copper-coated glass plate were used to characterize the composition versus radial position using a JEOL JXA-8200 Superprobe, equipped with an X-Y translation stage.

Electrodes deposited on Cu foil disks were assembled into 2325 coin cells with Li metal (99.9%, Sigma-Aldrich) counter electrodes and 1 M $LiPF_6$ (BASF) in EC/DEC/FEC (3:6:1 v/v/v, Novolyte Technologies) electrolyte in an Ar-filled glove box. The electrodes were separated by two layers of Celgard 2301 separator. Cells were cycled at 30 ± 0.1°C with a Maccor Series 4000 Automated Test System from 0.005 to 0.9 V at a C/10 rate and trickle discharged (lithiation) at 0.005 V to a C/40 rate in the first cycle. For subsequent cycles, cells were cycled from 0.005 to 0.9 V at a C/5 rate and trickle discharged at 0.005 V to a C/20 rate. The C-rate was calculated assuming all Si is active and all B is inactive.

Results and Discussion

Figure 1 shows the theoretical and measured composition for $Si_{1-x}B_x$ Library I as a function of position. The top panel shows the theoretical composition calculated from the linear variation of B and constant Si. The middle panel shows the atomic fractions of Si and

*Electrochemical Society Student Member.
**Electrochemical Society Active Member.
[z]E-mail: mnobrovac@dal.ca

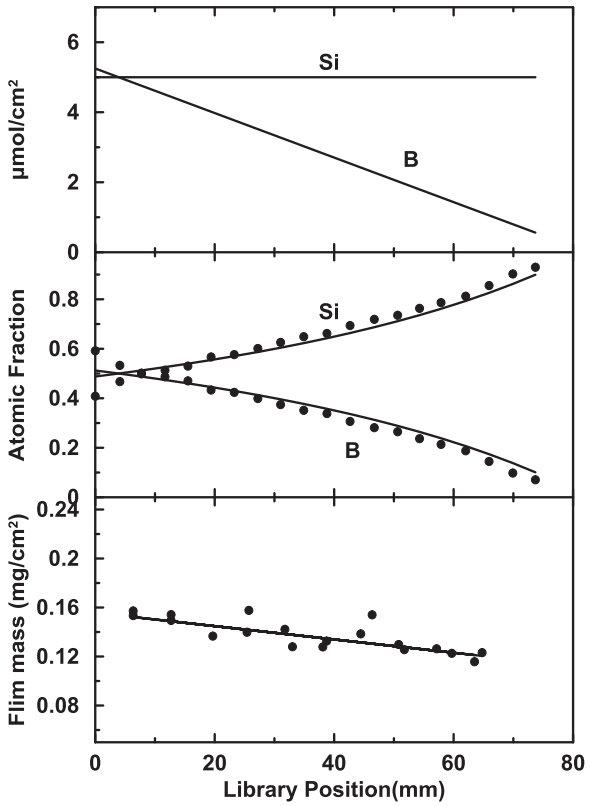

Figure 1. Theoretical and measured compositions of the $Si_{1-x}B_x$ Library I. The top panel shows the calculated Si and B moles per unit area defined by the "constant" and "linear out" sputtering masks. The middle panel shows that compositions calculated from the top panel agree with the measured compositions from electron microprobe. The bottom panel shows that the calculated mass per weighing disk (based on the top panel) agrees with the measured mass.

B as measured by electron microprobe and are in good agreement with that calculated in the top panel. The bottom panel shows that the measured mass of the sputtered films fits well with the calculated mass of the Cu foil disks. This shows that the compositions measured by electron microprobe and by mass are completely consistent with each other. A similar analysis has also been conducted to determine the composition range obtained in Library II. Table I lists the sputtering parameters and the composition range obtained for each Library. $Si_{1-x}B_x$ compositions of $0.071 < x < 0.592$ are obtained from Library I, and $0.379 < x < 0.950$ from Library II.

Figure 2 shows XRD patterns collected from 20 different positons on $Si_{1-x}B_x$ Library I with the values of x for each pattern indicated on the right hand side vertical axis. It is clear that no crystalline diffraction peaks occur in all patterns, indicating that the $Si_{1-x}B_x$ films are characteristic of a highly amorphous nature for all compositions on $Si_{1-x}B_x$ Library I. Similar results were found for Library II. Figure 3 shows selected XRD patterns of $Si_{0.929}B_{0.071}$, $Si_{0.694}B_{0.306}$, and $Si_{0.408}B_{0.592}$ from Library I. All these patterns have a main broad peak from 25° to 40°, and three other weak broad peaks centered approximately at 21°, 48° and 57°, respectively. These diffraction peaks are roughly

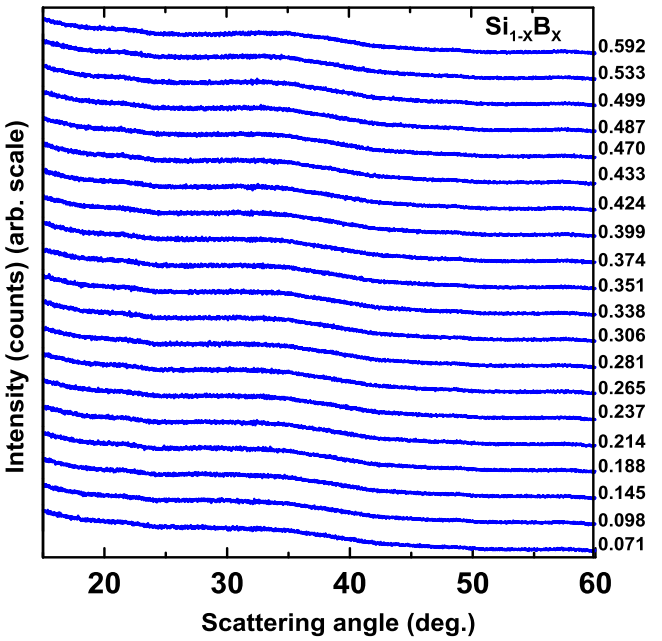

Figure 2. XRD patterns collected from different 20 positions of $Si_{1-x}B_x$ films (Library I) with the values of x for each pattern indicated on the right hand side vertical axis.

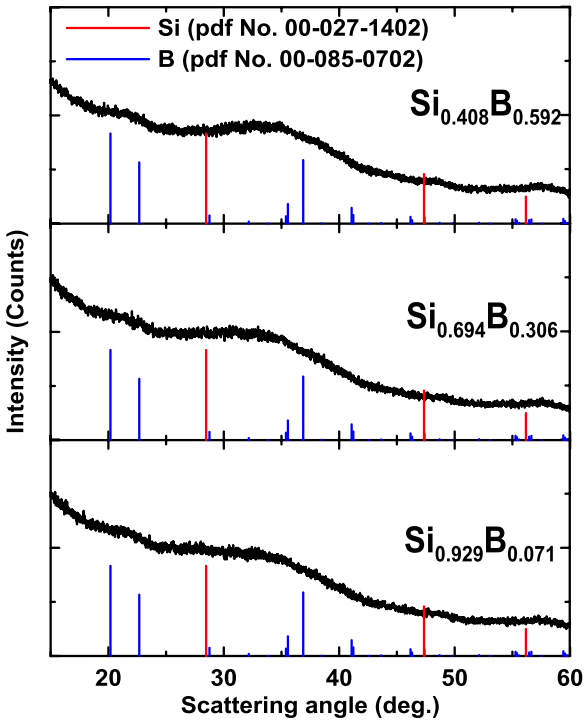

Figure 3. Selected XRD patterns of $Si_{0.929}B_{0.071}$, $Si_{0.694}B_{0.306}$, and $Si_{0.408}B_{0.592}$ films from Figure 2.

Table I. Summary of the sputtered libraries presented in this work.

	Deposition Power (w)		Covered Mask		
Library	Si	B	Si	B	Film composition (at%)
I	110	150	Constant	Linear In	$0.071 \leq x \leq 0.592$
II	110	150	Linear In	Constant	$0.379 \leq x \leq 0.950$

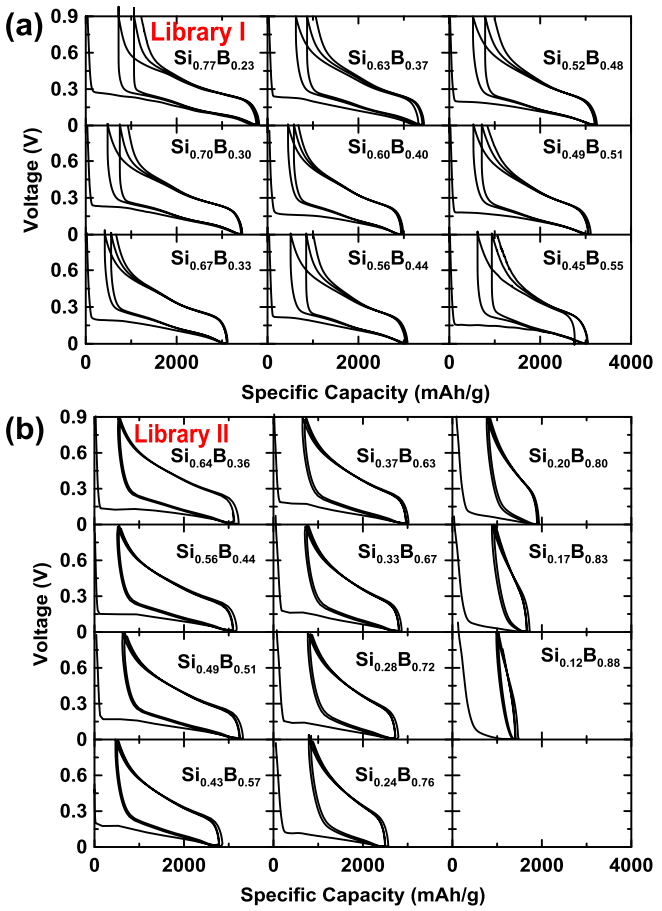

Figure 4. Voltage curves of $Si_{1-x}B_x$ versus lithium metal. The compositions of the films are indicated in the figure.

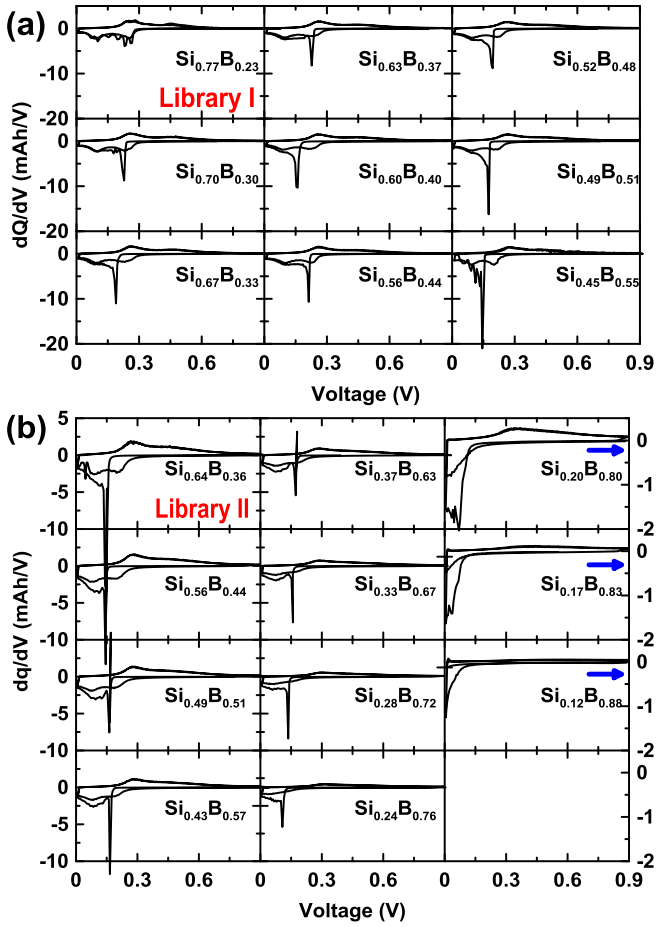

Figure 5. Differential capacity vs. potential curves for the first two cycles of $Si_{1-x}B_x$.

correlated with the peak positions of B (pdf No. 00-085-0702) and Si (pdf No. 00-027-1402). However, all the peaks in the XRD patterns that can be attributed to Si are shifted to higher angles. This may be related to a lattice constant decrease of Si resulted by B substitution.[20,24] These results suggest that the sputtered films are composed of an amorphous Si-rich Si-B solid solution that co-exists with amorphous boron. This is different from the Si-transition metal systems, in which the active Si phase coexists with metal silicides.[10–15]

Figures 4a and 4b show voltage curves of the first three cycles of $Si_{1-x}B_x$ electrodes cycled versus lithium metal between 0.005 to 0.9 V for Library I and Library II, respectively. All the voltage curves are characteristic of sputtered pure Si films, having an initial flat first discharge plateau and two pairs of sloping plateaus during the subsequent lithiation and delithiation process.[25–26] No plateau related to $Li_{15}Si_4$ is present during these initial cycles, which is consistent with Si films where $Li_{15}Si_4$ formation can be suppressed by the stress between the Si film and the substrate.[27] With increasing B concentration, both sloping plateaus shorten gradually so that the reversible capacity of $Si_{1-x}B_x$ electrode decreases. Nevertheless, $Si_{1-x}B_x$ electrodes with more than 80 at% B content still show obvious lithium storage capability. This is in contrast to Si-M (M = Fe, Ni, Mn) systems in which an inactive silicide phase is formed. Such Si-M alloys generally become inactive when the atomic percentage of M is greater than 40%.[11,16] This is further evidence that no inactive Si-B phase is formed in the current system and will be further confirmed below.

Figure 5 shows the differential capacity versus potential curves for the first two cycles of $Si_{1-x}B_x$ electrode derived from the voltage curves. It is clear to see that the shape of the differential capacity curves is characteristic of sputtered pure Si film and is hardly affected by B content when x is up to 0.76 in $Si_{1-x}B_x$.[25–26] No sharp peak exists during charge corresponding to $Li_{15}Si_4$ formation in all $Si_{1-x}B_x$ electrodes. The sharp peak during the first lithiation is characteristic of an initial nucleation and growth process, and its position shifts negatively from 0.23 V in $Si_{0.70}B_{0.30}$ to 0.14 V in $Si_{0.45}B_{0.55}$ in Library I. This suggests that B substitution somehow inhibits this process. In addition, two pairs of broad peaks correspond to high-voltage and low-voltage lithiation and delithiation for amorphous Si in the second cycle.[2] This suggests that amorphous Si seems to be the only active phase in $Si_{1-x}B_x$ thin films.

Figure 6 shows the initial reversible capacity versus x in $Si_{1-x}B_x$ films. Also shown are lines corresponding to the theoretical capacity of the Si-B alloys if all the Si is active (blue line, all Si forms $Li_{15}Si_4$, 3579 mAh/g, at full lithiation) or if inactive SiB_6 compounds were formed (brown line), as predicted by the Si-B phase diagram. For Library I with $0.379 \leq x \leq 0.950$, the reversible capacity of some $Si_{1-x}B_x$ films is a little lower than the theoretical capacity of all active Si, which can be recognized to be reasonable, since these samples have high volume expansion and would tend to suffer from mechanical failure, leading to capacity loss. At B contents above 50 at.%, the reversible capacity in $Si_{1-x}B_x$ films is in good agreement with all the Si being active, which coincides well with the XRD results. Therefore, $Si_{1-x}B_x$ alloy can be determined to consist of active amorphous Si (that likely contains some B in a solid solution) and inactive amorphous B.

Recently, we have reported that the average voltage of active Si/inactive transition metal silicide alloys can be shifted as a function of the amount of inactive phase. This voltage shift may be due to the stress induced by the active Si phase expanding while bonded to the inactive silicide phase.[16] Since stress from a substrate has also been reported to shift the voltage curve of thin film Si,[28] we speculate

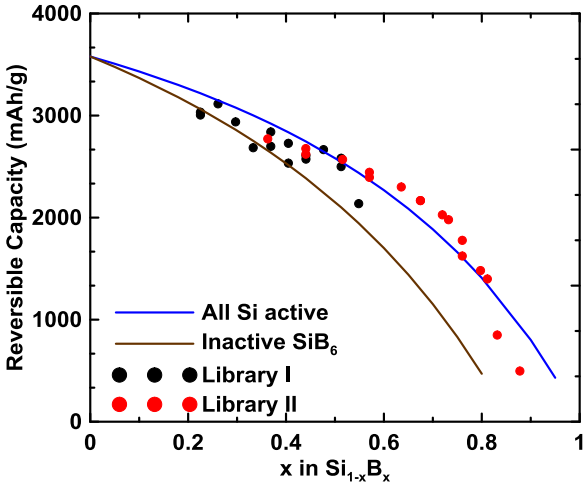

Figure 6. The first reversible capacity of $Si_{1-x}B_x$ films. Also shown are curves representing the theoretical capacity if all the Si is active and all the B is inactive or if the B reacts with Si to form inactive SiB_6.

that the voltage shifts observed in active Si/inactive phase alloys are related to how strongly the active Si is bonded to the inactive phase. To investigate if such a voltage shift occurs for Si-B alloys, Figure 7 shows the average voltage of the second lithiation and delithiation as a function of x in $Si_{1-x}B_x$. The average lithiation and delithiation voltage increase and decrease with x, respectively, in a linear manner up to a composition of about $x = 0.8$. This should be mainly induced by the negative/positive shift of lithiation/delithiation peaks, respectively, as shown in Figure 5. At higher B contents, the lower portion of the differential capacity becomes severely truncated. This would tend to cause the low voltage peak during delithiation to reduce in size, resulting in an increase in average delithiation voltage, as is observed in Figure 7. This phenomenon was also observed for Ni-Si alloys with high Ni content.[16] This does not explain, however why the average lithiation voltage should increase also when $x > 0.8$. Here, the capacities of the thin films are small, so that effects of cell capacitance and/or electrolyte reactions may be becoming significant. Indeed the differential capacities become featureless at these higher B contents and resemble capacitive charging.

Overall, the average voltage shift observed for B is much less than we have observed for Si-Ni alloys[16] and Si-Fe alloys.[29] Considering that the voltage shift has been associated with how strongly the inactive phase bonds to the active Si-phase,[16] this may be indicative

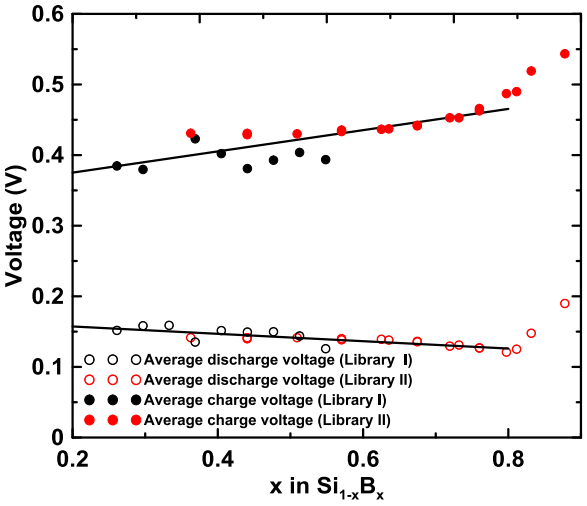

Figure 7. Average lithiation and delithiation voltage versus x in $Si_{1-x}B_x$ films.

that the Si-phase in Si-B alloys is bonded relatively weakly to the inactive B phase. A weakly bonded Si active phase has been shown to result in $Li_{15}Si_4$ formation and fade during cycling in thin films.[27] We will explore the longer-term cycling implications of this potentially weak interaction in a later publication using Si-B made by mechanical milling.

Conclusions

In this work, amorphous $Si_{1-x}B_x$ films have been obtained by magnetron sputtering and the effect of B concentration on the structure and electrochemical performance in $Si_{1-x}B_x$ films has been investigated as Li-ion negative electrodes. The XRD results indicate that sputtered $Si_{1-x}B_x$ is an amorphous mixture of Si (including Si-rich Si-B solid solution) and B. The voltage curves and differential capacity profiles of $Si_{1-x}B_x$ films are similar with that of sputtered pure Si, and the specific capacity corresponds to all the Si being active with lithium and the B being an inactive phase. Therefore, a Si/B active/inactive structure can be obtained in Si-B films for lithium ion anodes. Increasing x in $Si_{1-x}B_x$, results in the average lithiation and delithiation voltages to be shifted to lower and higher values, respectively. This is consistent with stress-voltage coupling from the expansion of the active Si phase while connected to the inactive and fixed B phase. However the magnitude of the shift is small, in comparison to the voltage shift induced by transition metals in Si-M alloys and may indicate a weak interaction between the active Si phase and inactive B phase in Si-B alloys.

Acknowledgments

The authors acknowledge funding from NSERC and 3M Canada, Co. under the auspices of the Industrial Research Chair and Discovery grant programs. We also acknowledge the support of other partners that fund the Facilities for Materials Characterization managed by the Institute for Research in Materials. Hui Liu acknowledges the support from Chinese Scholarship Council.

References

1. M. N. Obrovac and L. Christensen, *Electrochem. Solid-State Lett.*, **7**, A93 (2004).
2. M. N. Obrovac and L. J. Krause, *J. Electrochem. Soc.*, **154**(2), A103 (2007).
3. L. Baggetto, R. A. H. Niessen, F. Roozeboom, and P. H. L. Notten, *Adv. Funct. Mater.*, **18**, 1057 (2008).
4. F. Zhou, X. Zhao, P. P. Fergusoń, J. S. Thorne, R. A. Dunlap, and J. R. Dahn, *J. Electrochem. Soc.*, **155**, A921 (2008).
5. S-M. Hwang, H-K. Lee, S-W. Jang, S-M. Lee, S-J. Lee, H-K. Baik, and J-Y. Lee, *Electrochem. Solid-State Lett.*, **4**(7), A97 (2001).
6. T. D. Hatchard and J. R. Dahn, *J. Electrochem. Soc.*, **152**(7), A1445 (2005).
7. T. D. Hatchard, M. N. Obrovac, and J. R. Dahn, *J. Electrochem. Soc.*, **152**(12), A2335 (2005).
8. T. D. Hatchard and J. R. Dahn, *J. Electrochem. Soc.*, **151**(10), A1628 (2004).
9. T. D. Hatchard, M. N. Obrovac, and J. R. Dahn, *J. Electrochem. Soc.*, **153**(2), A282 (2006).
10. X. Zhao, R. A. Dunlap, and M. N. Obrovac, *J. Electrochem. Soc.*, **161**(14), A1976 (2014).
11. M. Fleischauer, J. Topple, and J. R. Dahn, *Electrochem. Solid-State Lett.*, **8**, A137 (2005).
12. H. Y. Lee and S. M. Lee, *J. Power Sources*, **112**, 649 (2002).
13. M. D. Fleischauer, J. M. Topple, and J. R. Dahn, *Electrochem. Solid St.*, **8**(2), A137 (2005).
14. M. D. Fleischauer, R. Mar, and J. R. Dahn, *J. Electrochem. Soc.*, **154**(3), A151 (2007).
15. G. X. Wang, L. Sun, D. H. Bradhurst, S. Zhong, S. X. Dou, and H. K. Liu, *J. Power Sources*, **88**, 278 (2000).
16. Z. Du, T. D. Hatchard, R. A. Dunlap, and M. N. Obrovac, *J. Electrochem. Soc.*, **162**, A1858 (2015).
17. S. Rousselot, M. Gauthier, D. Mazouzi, B. Lestriez, D. Guyomard, and L. Roué, *J. Power Sources*, **202**, 262 (2012).
18. A. Netz, R. A. Huggins, and W. Weppner, *J. Power Sources*, **119**, 95 (2003).
19. A. Netz and R A. Huggins, *Solid State Ionics*, **175**, 215 (2004).
20. R. Yi, J. Zai, F. Dai, M. L. Gordin, and D. Wang, *Electrochem. Commun.*, **36**, 29 (2013).
21. A. D. W. Todd, R. E. Mar, and J. R. Dahn, *J. Electrochem. Soc.*, **154**, A597 (2007).
22. J. S. Thorne, J. R. Dahn, M. N. Obrovac, and R. A. Dunlap, *J. Alloy. Comp.*, **509**, 6705 (2011).
23. Peng Liao, Bretton L. MacDonald, R. A. Dunlap, and J. R. Dahn, *Chem. Mater.*, **20**, 454 (2008).

24. J. M. Baribeau and S. J. Rolfe, *Appl. Phys. Lett.*, **58**, 2129 (1991).
25. J. P. Maranchi, A. F. Hepp, and P. N. Kumta, *Electrochem. Solid-State Lett.*, **6**, A198 (2003).
26. T. D. Hatchard, J. R. Dahn, S. Trussler, M. Fleischauer, A. Bonakdarpour, J. R. Mueller-Neuhaus, and K. C. Hewitt, *Thin Solid Films*, **443**, 144 (2003).
27. D. S. M. Iaboni and M. N. Obrovac, submitted to *J. Electrochem. Soc.*, August 1, 2015.
28. V. A. Sethuraman, V. Srinivasan, A. F. Bower, and P. R. Guduru, *J. Electrochem. Soc.*, **157**(11), A1253 (2010).
29. Zhijia Du, S. Ellis, R. A. Dunlap, and M. N. Obrovac, in preparation.